

Graphical Matrices in Chemistry*

Sonja Nikolić,** Ante Miličević, and Nenad Trinajstić

The Rugjer Bošković Institute, P. O. Box 180, HR-10002 Zagreb, Croatia

RECEIVED FEBRUARY 1, 2005; REVISED MARCH 1, 2005; ACCEPTED MARCH 8, 2005

Keywords
chemical graph theory
double invariants
graphical matrices
Hosoya-Wiener index
molecular descriptors
structure-property modeling
Wiener-Wiener index

Graphical matrices are presented. Their construction *via* selected sets of subgraphs and the replacement of subgraphs by numbers representing graph invariants are discussed. The last step of the procedure is applying the method of choice to obtain the desired double invariant from the graphical matrix in the numerical form. It is also pointed out that many so-called special graph-theoretical matrices from the literature are rooted in the corresponding graphical matrices. As examples of double invariants, two descriptors, the Wiener-Wiener index and the Hosoya-Wiener index, have been generated from the appropriate graphical matrices and used in the structure-boiling point and structure-steric energy modeling of octanes. The obtained models possess statistical parameters comparable to those of the best structure-boiling point and structure-steric energy models for octanes in the literature.

INTRODUCTION

Graphical matrices are matrices whose elements are subgraphs of the graph rather than numbers. Since the elements of these matrices are (sub)graphs, they are called graphical matrices.¹ Thus far, very little work has been reported on these matrices.^{1,2} However, many of the so-called special matrices,³ such as the Wiener matrices^{4–6} and the Hosoya matrices,⁷ may be regarded as the numerical realizations of the corresponding graphical matrices.

The advantage of a graphical matrix lies in the fact that it allows many possibilities of numerical realizations. In order to obtain a numerical form of a graphical matrix, one needs to select a graph invariant and replace all the graphical elements (subgraphs of some form) by the corresponding numerical values of the selected invariant. In this way, the numerical form of the graphical

matrix is established and one can select another or the same type of invariant – this time an invariant of the numerical matrix. Graph invariants generated in this way are double invariants² in view of the fact that two invariants are used in constructing a given molecular descriptor.

CONSTRUCTION OF GRAPHICAL MATRICES

There are two ways of constructing graphical matrices, denoted by \mathbf{M} , which lead to four types of these matrices. One way is to define the elements of the graphical matrix $[\mathbf{M}]_{ij}$ as the subgraphs obtained after consecutive removal of the edges connecting vertices i and j from graph G . We denote this kind of graphical matrices by ${}^e\mathbf{M}$, where e stands for the edge, and we call them the edge-graphical matrices. Matrix ${}^e\mathbf{M}$ is necessarily a sparse matrix, since it contains only a few non-vanishing el-

* Dedicated to our dear friend and colleague Edward C. Kirby on the occasion of his 70th birthday.

** Author to whom correspondence should be addressed. (E-mail: sonja@irb.hr)

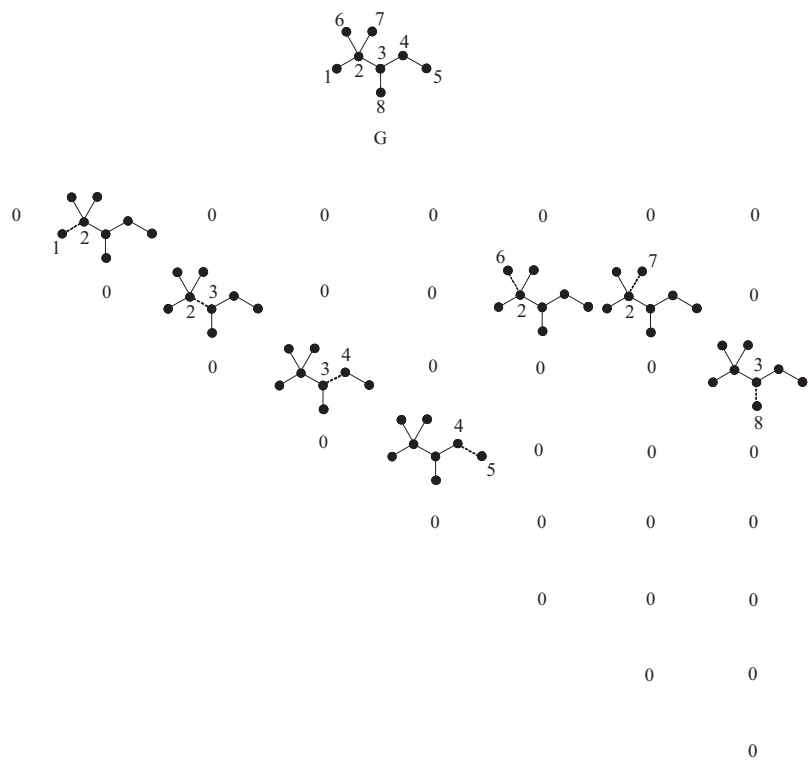


Figure 1. The edge-graphical matrix of G depicting the carbon skeleton of 2,2,3-trimethylpentane.

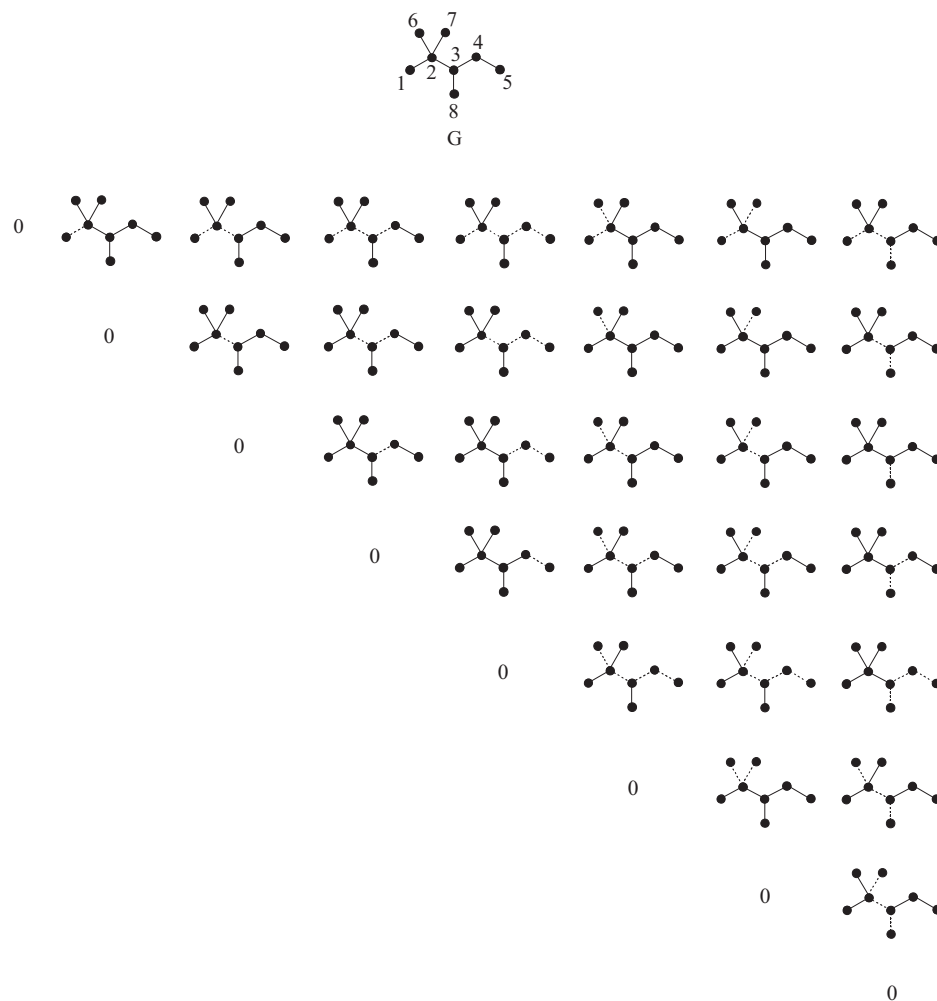


Figure 2. The path-graphical matrix of G depicting the carbon skeleton of 2,2,3-trimethylpentane.

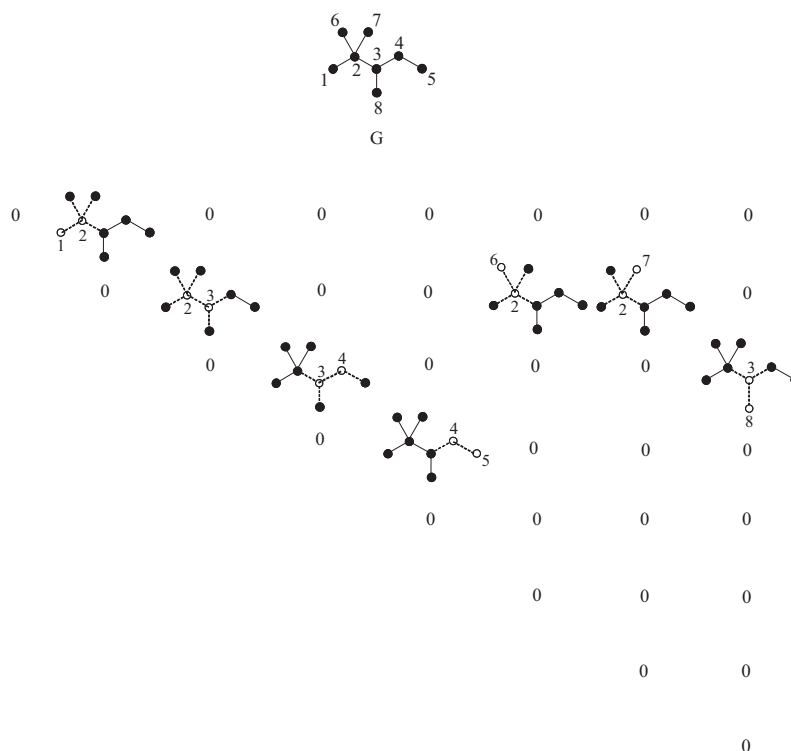


Figure 3. The sparse vertex-graphical matrix of G depicting the carbon skeleton of 2,2,3-trimethylpentane.

elements corresponding to the removed edges. An example of this kind of graphical matrix is given in Figure 1. Since the graphical matrix is a square, $V \times V$, symmetrical matrix ($V =$ the total number of vertices of G), it is enough for demonstrative purposes to give only the upper triangle of the matrix. For graphs without loops, the corresponding graphical matrices have zeros as diagonal elements.

If, however, we generate the graphical matrix by consecutive removal of the paths joining vertices i and j instead of edges, the obtained matrix is dense. We call this matrix the path-graphical matrix and denote it by ${}^p\mathbf{M}$. An illustrative example of a path-graphical matrix is given in Figure 2.

The second way of constructing graphical matrices is to define their elements $[\mathbf{M}]_{ij}$ as the subgraphs obtained after consecutive removal of adjacent vertices i and j , and the incident edges from graph G . The obtained graphical matrices are necessarily sparse matrices, since they contain only a few non-vanishing elements corresponding to the deleted adjacent vertices. We denote this kind of graphical matrices by ${}^{su\vee}\mathbf{M}$, where s denotes the sparse matrix and uv stands for the adjacent vertices, and we call these matrices the sparse vertex-graphical matrices. An example of such a matrix is given in Figure 3.

If, instead of considering only adjacent vertices, we consider pairs of vertices u and v at increasing distances, the obtained graphical matrix is dense, that is, all its matrix-elements but the diagonal elements are non-zero. We denote this matrix by ${}^{du\vee}\mathbf{M}$, where d denotes the dense matrix, and call it the dense vertex-graphical ma-

trix. Figure 4 displays the dense vertex-graphical matrix for the hydrogen-depleted graph G of 2,2,3-trimethylpentane.

NUMERICAL REALIZATION OF GRAPHICAL MATRICES

The next step is to replace (sub)graphs with the invariants of choice. In our case, we selected for illustrative purposes the Wiener index⁸⁻¹¹ and the Hosoya index.¹² The numbers that replace the subgraphs in the graphical matrices are obtained by summing up their Wiener indices or their Hosoya indices. Values of the Wiener indices and Hosoya indices for subgraphs are taken from our book on computational chemical graph theory.¹³ Below are the numerical realizations of all four graphical matrices presented in Figures 1-4.

The first numerical matrix, when the Wiener index is employed, is named the edge-Wiener matrix and denoted by ${}^e\mathbf{W}$. An example of this matrix obtained from the edge-graphical matrix of 2,2,3-trimethylpentane (see Figure 1) is given below. Only the upper triangle of the matrix is shown.

0	46	0	0	0	0	0	0
	0	19	0	0	46	46	0
		0	29	0	0	0	46
			0	42	0	0	0
				0	0	0	0
					0	0	0
						0	0
							0

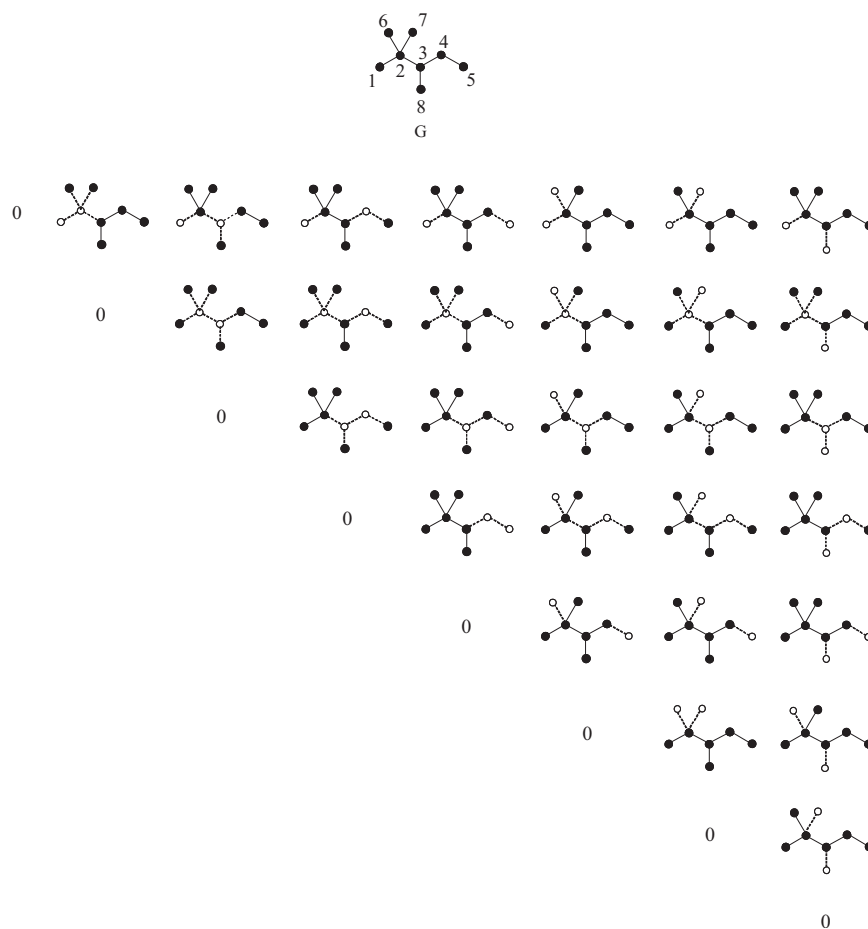


Figure 4. The dense vertex-graphical matrix of G depicting the carbon skeleton of 2,2,3-trimethylpentane.

Summation of the matrix-elements in the above matrix-triangle gives the edge-Wiener-Wiener index eWW of 2,2,3-trimethylpentane (${}^eWW = 274$).

If, however, we replace elements in the edge-Wiener matrix by the product of the number of vertices in each subgraph, the obtained numerical matrix, called in the literature the Wiener matrix,⁴⁻⁶ gives the standard Wiener index, usually denoted by W .¹⁴ This is valid only for acyclic graphs.

$$\begin{array}{cccccccc}
 0 & 7 & 0 & 0 & 0 & 0 & 0 & 0 \\
 0 & 16 & 0 & 0 & 7 & 7 & 0 & \\
 & 0 & 12 & 0 & 0 & 0 & 7 & \\
 & & 0 & 7 & 0 & 0 & 0 & \\
 & & & 0 & 0 & 0 & 0 & \\
 & & & & 0 & 0 & 0 & \\
 & & & & & 0 & 0 & \\
 & & & & & & 0 & \\
 & & & & & & & 0
 \end{array}$$

$W = 63$

If we select the Hosoya Z -index¹² instead of the Wiener index, the corresponding edge-Hosoya matrix, also known in the literature as the Hosoya Z matrix,⁷ is denoted by eZ . The Z -indices of subgraphs are also taken from our book¹³ and summed up to give the elements of the matrix.

$$\begin{array}{cccccccc}
 0 & 18 & 0 & 0 & 0 & 0 & 0 & 0 \\
 & 0 & 9 & 0 & 0 & 18 & 18 & 0 \\
 & & 0 & 11 & 0 & 0 & 0 & 15 \\
 & & & 0 & 14 & 0 & 0 & 0 \\
 & & & & 0 & 0 & 0 & 0 \\
 & & & & & 0 & 0 & 0 \\
 & & & & & & 0 & 0 \\
 & & & & & & & 0
 \end{array}$$

Summation of the matrix-elements in the above matrix-triangle gives the edge-Hosoya-Wiener index eZW of 2,2,3-trimethylpentane (${}^eZW = 107$).

The second numerical matrix, if the Wiener index is employed, is named the path-Wiener matrix and is denoted by pW . An example of this matrix obtained from the path-graphical matrix of 2,2,3-trimethylpentane (see Figure 2) is given below and again only the upper triangle of the matrix is shown.

$$\begin{array}{cccccccc}
 0 & 46 & 14 & 6 & 5 & 31 & 31 & 8 \\
 & 0 & 19 & 11 & 10 & 46 & 46 & 13 \\
 & & 0 & 29 & 28 & 14 & 14 & 46 \\
 & & & 0 & 42 & 6 & 6 & 17 \\
 & & & & 0 & 5 & 5 & 16 \\
 & & & & & 0 & 31 & 8 \\
 & & & & & & 0 & 8 \\
 & & & & & & & 0
 \end{array}$$

Summation of the matrix-elements in the above matrix-triangle gives the path-Wiener-Wiener number PWW of 2,2,3-trimethylpentane (${}^PWW = 561$).

Note, if we replace the elements in the path-Wiener matrix by the product of the numbers of vertices in each subgraph, the obtained numerical matrix gives the hyper-Wiener index,^{4,5,15} which we denote by hW . This is valid only for acyclic graphs.

0	7	12	12	6	6	6	9
	0	16	16	8	7	7	12
		0	12	6	12	12	7
			0	7	12	12	10
				0	6	6	5
					0	6	9
						0	9
							0

$${}^hW = 255$$

This way of computing the hyper-Wiener index for acyclic structures is much simpler than the usual way.⁴

If we select the Hosoya Z-index¹² instead of the Wiener index, the corresponding path-Hosoya matrix is denoted by PZ . The Z-indices of subgraphs are also taken from our book.¹³

0	18	9	8	8	14	14	8
	0	9	8	8	18	18	8
		0	11	11	9	9	15
			0	14	8	8	8
				0	8	8	8
					0	14	8
						0	8
							0

Summation of the matrix-elements in the above matrix-triangle gives the path-Hosoya-Wiener index PZW of 2,2,3-trimethylpentane (${}^PZW = 295$).

The third numerical matrix, if the Wiener index is employed, is named the sparse vertex-Wiener matrix and is denoted by ${}^{suv}W$. An example of this matrix obtained from the sparse vertex-graphical matrix of 2,2,3-trimethylpentane (see Figure 3) is given below. Only the upper triangle of the matrix is shown.

0	10	0	0	0	0	0	0
	0	1	0	0	10	10	0
		0	9	0	0	0	10
			0	28	0	0	0
				0	0	0	0
					0	0	0
						0	0
							0

Summation of the matrix-elements in the above matrix-triangle gives the sparse vertex-Wiener-Wiener index ${}^{suv}WW$ of 2,2,3-trimethylpentane (${}^{suv}WW = 78$).

If we select the Hosoya Z-index¹² instead of the Wiener index, the corresponding sparse vertex-Hosoya matrix is denoted by ${}^{suv}Z$. The Z-indices of subgraphs are also taken from our book¹³ and summed up to give the elements of the matrix.

0	7	0	0	0	0	0	0
	0	6	0	0	7	7	0
		0	6	0	0	0	6
			0	9	0	0	0
				0	0	0	0
					0	0	0
						0	0
							0

Summation of the matrix-elements in the above matrix-triangle gives the sparse vertex-Hosoya-Wiener index ${}^{suv}ZW$ of 2,2,3-trimethylpentane (${}^{suv}ZW = 48$).

The fourth numerical matrix, if the Wiener index is employed, is named the dense vertex-Wiener matrix, denoted by ${}^{duv}W$. An example of this matrix obtained from the dense vertex-graphical matrix of 2,2,3-trimethylpentane (see Figure 4) is given below. Only the upper triangle of the matrix is shown.

0	10	5	18	29	31	31	32
	0	1	1	4	10	10	4
		0	9	9	5	5	10
			0	28	18	18	16
				0	29	29	28
					0	31	32
						0	32
							0

Summation of the matrix-elements in the above matrix-triangle gives the dense vertex-Wiener-Wiener index ${}^{duv}WW$ of 2,2,3-trimethylpentane (${}^{duv}WW = 485$).

If we select the Hosoya Z-index¹² instead of the Wiener index, the corresponding dense vertex-Hosoya matrix is denoted by ${}^{duv}Z$. The Z-indices of subgraphs are also taken from our book.¹³

0	7	6	8	10	12	12	11
	0	6	6	6	7	7	6
		0	6	6	6	6	6
			0	9	6	8	6
				0	10	10	9
					0	12	11
						0	11
							0

Summation of the matrix-elements in the above matrix-triangle gives the dense vertex-Hosoya-Wiener index ${}^{\text{duv}}ZW$ of 2,2,3-trimethylpentane (${}^{\text{duv}}ZW = 226$).

It should be noted that the Wiener matrix and the Hosoya matrix have not been connected previously with graphical matrices.

A GENERALIZED METHOD FOR CONSTRUCTING GRAPHICAL MATRICES AND OBTAINING THE RELATED MOLECULAR DESCRIPTORS

The above procedure may be generalized as follows:

- (i) Representation of the molecule by the corresponding hydrogen-depleted graph;
- (ii) Labeling of the vertices;
- (iii) Construction of the sparse graphical matrix by consecutively removing edges or adjacent vertices from the graph;
- (iv) Construction of the dense graphical matrix by consecutively removing paths of a given length or pairs of end-vertices of paths from the graph;
- (v) Replacing the elements of sparse and dense graphical matrices by numerical values of the selected graph invariants to obtain the corresponding numerical matrices, that is, matrices with numerical elements;
- (vi) Applying a graph invariant of choice to the numerical matrix;
- (vii) Getting a double invariant of a graph.

TABLE I. Values of the Wiener index (W) and the four Wiener-Wiener indices (${}^{\text{e}}WW$, ${}^{\text{p}}WW$, ${}^{\text{suv}}WW$, ${}^{\text{duv}}WW$) of octanes

Octanes ^(a)	W	${}^{\text{e}}WW$	${}^{\text{p}}WW$	${}^{\text{suv}}WW$	${}^{\text{duv}}WW$
n-octane	84	252	504	140	378
2-M-heptane	79	262	509	118	398
3-M-heptane	76	268	520	121	416
4-M-heptane	75	270	525	122	423
3-E-hexane	72	276	536	134	441
2,2-MM-hexane	71	270	561	88	438
2,3-MM-hexane	70	274	524	104	449
2,4-MM-hexane	71	274	521	102	443
2,5-MM-hexane	74	270	512	98	423
3,3-MM-hexane	67	274	595	94	464
3,4-MM-hexane	68	276	528	106	462
3,2-EM-pentane	67	278	533	116	469
3,3-EM-pentane	64	276	624	102	483
2,2,3-MMM-pentane	63	274	561	78	485
2,2,4-MMM-pentane	66	274	558	72	467
2,3,3-MMM-pentane	62	274	586	80	491
2,3,4-MMM-pentane	65	276	521	88	477
2,2,3,3-MMMM-butane	58	270	588	54	507

^(a)Abbreviations M and E denote methyl and ethyl, respectively.

TESTING THE WIENER-WIENER AND HOSOYA-WIENER INDICES

To exemplify the use of the double invariants, we applied the Wiener-Wiener and Hosoya-Wiener indices as predictor variables in modeling the boiling points, bp, and the total steric energies, SE, of octane isomers. In selecting octanes as a test set, we followed the advice of Randić.¹⁶ He recommended octanes as a test set because it consists of only 18 isomers possessing sufficient structural variations.

We give for octanes the original Wiener index and all four Wiener-Wiener indices in Table I and the original Hosoya index and all four Hosoya-Wiener indices in Table II. The boiling points¹⁷ (bp in °C) and the total steric energies¹⁸ (SE in kJ mol⁻¹) of octanes are given in Table III.

The structure-property modeling was carried out by the CROMRsel procedure.¹⁹⁻²¹ This is a multivariate procedure that has been designed to select the best possible model among the set of models obtained for a given number of descriptors, the criterion being the standard error of estimate. The quality of models is expressed by fitted (descriptive) statistical parameters: the correlation coefficient (R_{fit}), the standard error of estimate (S_{fit}) and Fisher's test (F). The models are also cross(internally)-validated by a leave-one-out procedure. Statistical parameters for the cross-validated models are symbolized by R_{cv} and S_{cv} , where subscript cv denotes the cross-validation.

TABLE II. Values of the Hosoya index (Z) and the four Hosoya-Wiener indices (${}^{\text{e}}ZW$, ${}^{\text{p}}ZW$, ${}^{\text{suv}}ZW$, ${}^{\text{duv}}ZW$) of octanes

Octanes ^(a)	Z	${}^{\text{e}}ZW$	${}^{\text{p}}ZW$	${}^{\text{suv}}ZW$	${}^{\text{duv}}ZW$
n-octane	34	106	250	64	216
2-M-heptane	29	106	259	47	215
3-M-heptane	31	110	273	60	223
4-M-heptane	30	110	274	58	224
3-E-hexane	32	116	286	65	232
2,2-MM-hexane	23	100	277	48	216
2,3-MM-hexane	27	110	284	54	228
2,4-MM-hexane	26	107	279	52	224
2,5-MM-hexane	25	104	266	50	218
3,3-MM-hexane	25	106	289	52	226
3,4-MM-hexane	29	114	296	58	234
3,2-EM-pentane	28	115	293	58	236
3,3-EM-pentane	28	114	312	60	237
2,2,3-MMM-pentane	22	103	289	48	228
2,2,4-MMM-pentane	19	94	268	42	216
2,3,3-MMM-pentane	23	106	298	50	232
2,3,4-MMM-pentane	24	108	292	50	232
2,2,3,3-MMMM-butane	17	92	278	42	222

^(a)Abbreviations M and E denote methyl and ethyl, respectively.

TABLE III. The boiling points (bp in °C) and the total steric energies (SE in kJ mol⁻¹) of octanes.

Octanes ^(a)	bp ^(b)	SE ^(c)
n-octane	125.7	0
2-M-heptane	117.6	2.5439
3-M-heptane	118.9	5.0877
4-M-heptane	117.7	5.0877
3-E-hexane	118.5	7.6316
2,2-MM-hexane	106.8	5.8450
2,3-MM-hexane	115.6	11.7905
2,4-MM-hexane	109.4	7.6316
2,5-MM-hexane	109.1	5.0877
3,3-MM-hexane	112.0	11.6901
3,4-MM-hexane	117.7	14.6984
3,2-EM-pentane	115.6	14.6984
3,3-EM-pentane	118.2	17.5351
2,2,3-MMM-pentane	109.8	18.7987
2,2,4-MMM-pentane	99.2	15.6607
2,3,3-MMM-pentane	114.8	22.0999
2,3,4-MMM-pentane	113.5	19.2380
2,2,3,3-MMMM-butane	106.5	27.2002

^(a)Abbreviations M and E denote methyl and ethyl, respectively.

^(b)Taken from G. Rücker and C. Rücker, *J. Chem. Inf. Comput. Sci.* **39** (1999) 788–802.

^(c)Taken from M. Randić, *J. Mol. Struct. (Theochem)* **233** (1991) 45–59.

We first considered the structure-boiling point modeling and the structure-steric energy modeling based only on the set of indices consisting of the Wiener index and Wiener-Wiener indices. In building these models, we considered all possible combinations between the indices from Table I, starting from a single index to up to four indices. We give statistical parameters (R_{fit} , S_{fit} , R_{cv} , S_{cv} , F) for the best structure-boiling point models in Ta-

ble IV and for the best structure-steric energy models in Table V.

We note that the best models do not include the Wiener index. Statistical parameters indicate that the structure-boiling point model ($R_{\text{fit}} = 0.54$, $S_{\text{fit}} = 5.3$ °C, $R_{\text{cv}} = 0.37$, $S_{\text{cv}} = 5.9$ °C, $F = 7$) and the structure-steric energy model ($R_{\text{fit}} = 0.958$, $S_{\text{fit}} = 2.2$ kJ mol⁻¹, $R_{\text{cv}} = 0.939$, $S_{\text{cv}} = 2.6$ kJ mol⁻¹, $F = 179$) based on the Wiener index are not as good as the models based on the Wiener-Wiener indices, though the performance of the Wiener index in the case of the structure-steric energy modeling is much better than when the Wiener index is used in the structure-boiling point modeling. However, it has been known for some time that the Wiener index is a poor descriptor to be used in structure-boiling point modeling based on a single descriptor.¹⁶ It appears that the best structure-boiling point model ($R_{\text{fit}} = 0.928$, $S_{\text{fit}} = 2.5$ °C, $R_{\text{cv}} = 0.868$, $S_{\text{cv}} = 3.3$ °C, $F = 29$) and the structure-steric energy model ($R_{\text{fit}} = 0.990$, $S_{\text{fit}} = 1.13$ kJ mol⁻¹, $R_{\text{cv}} = 0.985$, $S_{\text{cv}} = 1.4$ kJ mol⁻¹, $F = 241$) as the result of the CROMRsel procedure are both based on the three descriptors.

We next carried out the structure-boiling point modeling and the structure-steric energy modeling based only on the set of indices consisting of the Hosoya index and Wiener-Hosoya indices. In building these models we considered all possible combinations between the indices in Table II, starting from a single index to up to four indices. We give statistical parameters (R_{fit} , S_{fit} , R_{cv} , S_{cv} , F) for the best structure-boiling point models in Table VI and for the best structure-steric energy models in Table VII.

First we note that, unlike the models discussed above, some of the best models include the Hosoya index. Statistical parameters indicate that the structure-boiling point model ($R_{\text{fit}} = 0.887$, $S_{\text{fit}} = 2.9$ °C, $R_{\text{cv}} = 0.838$, $S_{\text{cv}} =$

TABLE IV. Statistical parameters R_{fit} , S_{fit} , R_{cv} , S_{cv} and F for the structure-boiling point model based on the Wiener index and the best structure-boiling point models with one, two, three and four Wiener-type indices. Note, $N = 18$ and $l = 1, \dots, 4$

Index	R_{fit}	R_{cv}	$S_{\text{fit}}(N - l - 1)$	$S_{\text{cv}}(N - l - 1)$	F
W	0.538	0.374	5.3	5.9	7
su ^v WW	0.811	0.744	3.7	4.2	31
su ^v WW, du ^v WW	0.842	0.734	3.5	4.3	18
e ^v WW, su ^v WW, du ^v WW	0.928	0.868	2.5	3.3	29
e ^v WW, p ^v WW, su ^v WW, du ^v WW	0.929	0.855	2.6	3.6	21

TABLE V. Statistical parameters R_{fit} , S_{fit} , R_{cv} , S_{cv} and F for the structure-steric energy model based on the Wiener index and the best structure-steric energy models with one, two, three and four Wiener-type indices. Note $N = 18$ and $l = 1, \dots, 4$

Index	R_{fit}	R_{cv}	$S_{\text{fit}}(N - l - 1)$	$S_{\text{cv}}(N - l - 1)$	F
W	0.958	0.939	2.2	2.6	179
du ^v WW	0.962	0.946	2.1	2.5	200
e ^v WW, du ^v WW	0.982	0.978	1.5	1.6	204
e ^v WW, p ^v WW, du ^v WW	0.990	0.985	1.13	1.4	241
e ^v WW, p ^v WW, su ^v WW, du ^v WW	0.992	0.982	1.09	1.6	195

TABLE VI. Statistical parameters R_{fit} , S_{fit} , R_{cv} , S_{cv} and F for the best structure-boiling point models with one, two, three and four Hosoya-type indices. Note $N = 18$ and $l = 1, \dots, 4$

Index	R_{fit}	R_{cv}	$S_{\text{fit}}(N - I - 1)$	$S_{\text{cv}}(N - I - 1)$	F
Z	0.887	0.838	2.9	3.4	59
Z, $^{\text{duv}}\text{ZW}$	0.906	0.830	2.8	3.6	34
Z, ZW, $^{\text{duv}}\text{ZW}$	0.940	0.892	2.3	3.0	36
Z, $^{\text{e}}\text{ZW}$, $^{\text{suv}}\text{ZW}$, $^{\text{duv}}\text{ZW}$	0.964	0.928	1.9	2.6	43

TABLE VII. Statistical parameters R_{fit} , S_{fit} , R_{cv} , S_{cv} and F for the best structure-steric energy models with one, two, three and four Hosoya type indices. Note $N = 18$ and $l = 1, \dots, 4$

Index	R_{fit}	R_{cv}	$S_{\text{fit}}(N - I - 1)$	$S_{\text{cv}}(N - I - 1)$	F
Z	0.703	0.615	5.5	6.1	17
$^{\text{e}}\text{ZW}$, $^{\text{duv}}\text{ZW}$	0.984	0.974	1.43	1.8	223
$^{\text{e}}\text{ZW}$, $^{\text{suv}}\text{ZW}$, $^{\text{duv}}\text{ZW}$	0.986	0.965	1.39	2.16	157
Z, $^{\text{e}}\text{ZW}$, $^{\text{suv}}\text{ZW}$, $^{\text{duv}}\text{ZW}$	0.994	0.984	1.0	1.5	253

3.4 °C, $F = 59$) based on the Hosoya index is better than one based on the Wiener index whilst the structure-steric energy model ($R_{\text{fit}} = 0.703$, $S_{\text{fit}} = 5.5$ kJ mol⁻¹, $R_{\text{cv}} = 0.615$, $S_{\text{cv}} = 6.1$ kJ mol⁻¹, $F = 16$) based on the Hosoya index is inferior to the model based on the Wiener index, as already observed by Randić *et al.*¹ The best structure-boiling point model ($R_{\text{fit}} = 0.964$, $S_{\text{fit}} = 1.9$ °C, $R_{\text{cv}} = 0.929$, $S_{\text{cv}} = 2.6$ °C, $F = 43$) contains four descriptors including the Hosoya index while a good structure-steric energy model ($R_{\text{fit}} = 0.984$, $S_{\text{fit}} = 1.4$ kJ mol⁻¹, $R_{\text{cv}} = 0.974$, $S_{\text{cv}} = 1.8$ kJ mol⁻¹, $F = 223$) is based on two descriptors not including the Hosoya index. The structure-steric energy model ($R_{\text{fit}} = 0.994$, $S_{\text{fit}} = 1.0$ kJ mol⁻¹, $R_{\text{cv}} = 0.984$, $S_{\text{cv}} = 1.5$ kJ mol⁻¹, $F = 253$) based on four descriptors including the Hosoya index is a rather unstable model.

Finally, we carried out the structure-boiling point modeling and the structure-steric energy modeling based

on the set of indices consisting of the Wiener and Hosoya indices, and Wiener-Wiener and Wiener-Hosoya indices. In building these models, we considered all the possible combinations between indices, starting from a single index to up to four indices. We give statistical parameters (R_{fit} , S_{fit} , R_{cv} , S_{cv} , F) for the best structure-boiling point models in Table VIII and for the best structure-steric energy models in Table IX.

The best structure-boiling point model is based on three descriptors, one being surprisingly the Wiener index. This is also the best overall structure-boiling point model:

$$\text{bp} = 324 (\pm 24) - 0.522 (\pm 0.081) W - 1.062 (\pm 0.084) ^{\text{e}}\text{WW} + 1.069 (\pm 0.056) ^{\text{e}}\text{ZW} \quad (1)$$

$$R_{\text{fit}} = 0.987 \quad S_{\text{fit}} = 1.09 \text{ °C} \quad R_{\text{cv}} = 0.978 \quad S_{\text{cv}} = 1.40 \text{ °C} \\ F = 173$$

TABLE VIII. Statistical parameters R_{fit} , S_{fit} , R_{cv} , S_{cv} and F for the best structure-boiling point models with one, two, three and four Wiener-type and Hosoya-type indices. Note $N = 18$ and $l = 1, \dots, 8$

Index	R_{fit}	R_{cv}	$S_{\text{fit}}(N - I - 1)$	$S_{\text{cv}}(N - I - 1)$	F
Z	0.887	0.838	2.9	3.4	59
$^{\text{e}}\text{WW}$, $^{\text{e}}\text{ZW}$	0.947	0.909	2.1	2.7	65
W, $^{\text{e}}\text{WW}$, $^{\text{e}}\text{ZW}$	0.987	0.978	1.09	1.4	173
W, $^{\text{e}}\text{WW}$, Z, $^{\text{e}}\text{ZW}$	0.989	0.978	1.05	1.5	142

TABLE IX. Statistical parameters R_{fit} , S_{fit} , R_{cv} , S_{cv} and F for the best structure-steric energy models with one, two, three and four Wiener-type and Hosoya-type indices. Note $N = 18$ and $l = 1, \dots, 8$

Index	R_{fit}	R_{cv}	$S_{\text{fit}}(N - I - 1)$	$S_{\text{cv}}(N - I - 1)$	F
$^{\text{duv}}\text{WW}$	0.962	0.946	2.1	2.5	200
$^{\text{e}}\text{ZW}$, $^{\text{duv}}\text{ZW}$	0.984	0.974	1.4	1.8	223
$^{\text{e}}\text{WW}$, $^{\text{P}}\text{WW}$, $^{\text{duv}}\text{WW}$	0.990	0.985	1.1	1.4	241
Z, $^{\text{e}}\text{ZW}$, $^{\text{suv}}\text{ZW}$, $^{\text{duv}}\text{WW}$	0.994	0.984	0.96	1.5	253

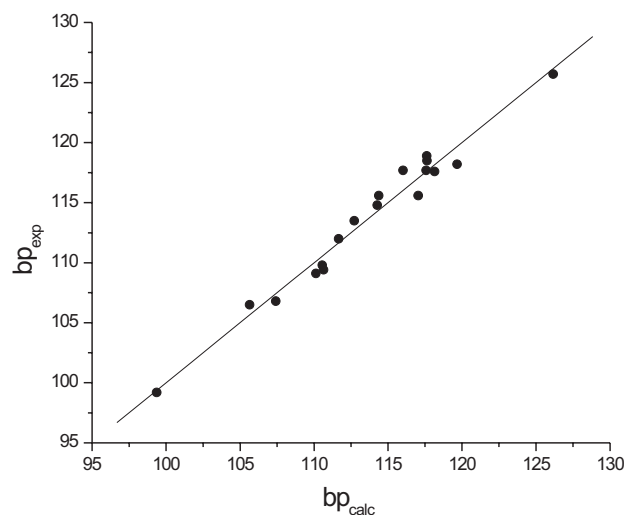


Figure 5. Scatter plot between the experimental and calculated octane boiling points for model (1).

In Figure 5, we give the scatter plot between the experimental and calculated values of octane boiling points for the above model.

Our structure-boiling point for octanes (1) is comparable with the best models in the literature. For example, the model based on the combination of *twc* (total walk count), $W^{0.25}$ (the fourth root of the Wiener index) and p_3 (the number of paths of length 3) has $R_{\text{fit}} = 0.996$ and $S_{\text{fit}} = 0.85$ °C.¹⁷

We selected as the best structure-steric energy model the one based on two descriptors. This is an equivalent to the model given in Table VII. We selected this model because it is stable and rests on only two parameters:

$$SE = 145.27 (\pm 10.87) - 1.27 (\pm 0.07) {}^cZW + 1.30 (\pm 0.06) {}^{\text{duv}}ZW \quad (2)$$

$$R_{\text{fit}} = 0.984 \quad S_{\text{fit}} = 1.4 \text{ kJ mol}^{-1} \quad R_{\text{cv}} = 0.974 \\ S_{\text{cv}} = 1.8 \text{ kJ mol}^{-1} \quad F = 223$$

In Figure 6, we give the scatter plot between the experimental and calculated values of octane steric energies for the model (2).

Our structure-steric energy model (2) is also comparable to the models from the literature. In their paper on what we call here the dense vertex-Wiener-Wiener index ${}^{\text{duv}}WW$, Randić *et al.*¹ collected 14 different quadratic regression models of total steric energies of octanes based on a variety of molecular descriptors with the standard errors of estimate for the fit models ranging from 1.29 kJ mol⁻¹ to 5.63 kJ mol⁻¹. All our models reported in Tables V, VII and IX fall within this range. Their own quadratic model, which is better than most, possesses the following statistical characteristics: $R_{\text{fit}} = 0.987$, $S_{\text{fit}} = 1.3$ kJ mol⁻¹ and $F = 272$. The model proposed by Ran-

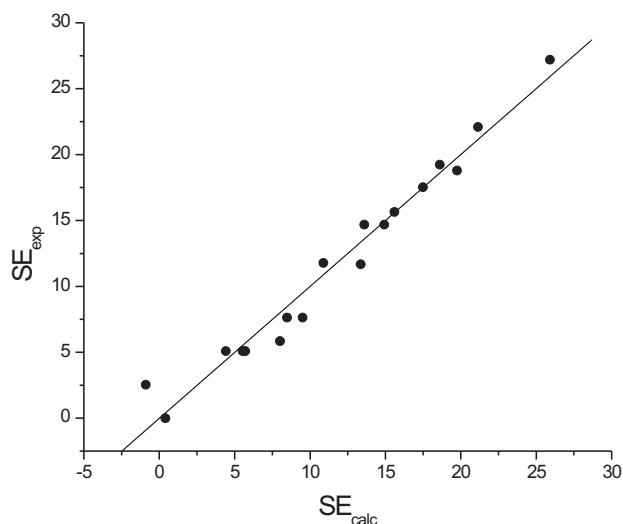


Figure 6. Scatter plot between the experimental and calculated octane total steric energies for model (2).

dić⁴ when he introduced the Wiener matrix is also a very good quadratic regression model, judging by its statistical characteristics: $R_{\text{fit}} = 0.984$, $S_{\text{fit}} = 1.4$ kJ mol⁻¹ and $F = 227$.

CONCLUSION

This paper belongs to our continuous efforts to construct graph invariants of chemical interest and to use them in the structure-property-activity modeling [*e.g.*, 22–26]. In the present article, we have discussed an approach for constructing a class of graph-theoretical matrices that are called graphical matrices. They can be used for generating double invariants. Thus far, double invariants have found limited use in QSPR and QSAR modeling. For example, they are only mentioned in passing in the monumental Todeschini and Consonni's *Handbook of Molecular Descriptors*.²⁷ In this report, the preliminary results show that the structure-property modeling based on the Wiener-Wiener and/or Hosoya-Wiener indices has potentials. Hence, further exploration of the graphical matrices and their invariants is warranted.

Acknowledgment. – This work was supported by Grant No. 0098034 of the Ministry of Science, Education and Sports of the Republic of Croatia.

REFERENCES

1. M. Randić, N. Basak, and D. Plavšić, *Croat. Chem. Acta* **77** (2004) 251–257.
2. M. Randić, D. Plavšić, and M. Razinger, *MATCH – Comm. Math. Comput. Chem.* **35** (1997) 243–259.
3. A. Miličević, S. Nikolić, N. Trinajstić, and D. Janežič, Graph-Theoretical Matrices in Chemistry, *Adv. Quantum Chem.*, in press. Reprints of this paper are available from sonja@irb.hr

4. M. Randić, *Chem. Phys. Lett.* **211** (1993) 478–483.
5. M. Randić, X. Guo, T. Oxley, and H. Krishnapryan, *J. Chem. Inf. Comput. Sci.* **33** (1993) 709–716.
6. M. Randić, X. Guo, T. Oxley, H. Krishnapryan, and L. Naylor, *J. Chem. Inf. Comput. Sci.* **34** (1994) 361–367.
7. M. Randić, *Croat. Chem. Acta* **67** (1994) 415–429.
8. H. Wiener, *J. Am. Chem. Soc.* **69** (1947) 19–20.
9. S. Nikolić, N. Trinajstić, and Z. Mihalić, *Croat. Chem. Acta* **68** (1995) 105–129.
10. A. A. Dobrynin, R. Entringer, and I. Gutman, *Acta Appl. Math.* **66** (2001) 211–249.
11. A. A. Dobrynin and L. S. Mel'nikov, *Croat. Chem. Acta* **77** (2004) 477–480.
12. H. Hosoya, *Bull. Chem. Soc. Jpn.* **45** (1972) 3415–3421.
13. N. Trinajstić, S. Nikolić, J. von Knop, W. R. Müller, and K. Szymanski, *Computational Chemical Graph Theory – Characterization, Enumeration and Generation of Chemical Structures by Computer Methods*, Horwood, New York, 1991, pp. 263–266.
14. N. Trinajstić, *Chemical Graph Theory*, 2nd revised ed., CRC Press, Boca Raton, Florida, 1992
15. O. Ivanciuc and T. Ivanciuc in: J. Devillers and A.T. Balaban, (Eds.) *Topological Indices and Related Descriptors in QSAR and QSPR*, Gordon & Breach, Amsterdam, 1999, pp. 221–277.
16. Randić, *Croat. Chem. Acta* **66** (1993) 289–312.
17. G. Rücker and C. Rücker, *J. Chem. Inf. Comput. Sci.* **39** (1999) 788–802.
18. M. Randić, *J. Mol. Struct. (Theochem)* **233** (1991) 45–59.
19. B. Lučić and N. Trinajstić, *J. Chem. Inf. Comput. Sci.* **39** (1999) 121–132.
20. T. Piližota, B. Lučić, and N. Trinajstić, *J. Chem. Inf. Comput. Sci.* **44** (2004) 113–121.
21. A. Miličević and S. Nikolić, *Croat. Chem. Acta* **77** (2004) 97–101.
22. Z. Mihalić, S. Nikolić, and N. Trinajstić, *J. Chem. Inf. Comput. Sci.* **32** (1992) 28–37.
23. Z. Mihalić and N. Trinajstić, *J. Chem. Educ.* **69** (1992) 701–712.
24. M. Randić and N. Trinajstić, *J. Mol. Struct. (Theochem)* **300** (1993) 551–572.
25. D. Amić, D. Davidović-Amić, D. Bešlo, and N. Trinajstić, *Croat. Chem. Acta* **76** (2003) 55–61.
26. S. Nikolić, G. Kovačević, A. Miličević, and N. Trinajstić, *Croat. Chem. Acta* **76** (2003) 113–124.
27. R. Todeschini and V. Consonni, *Handbook of Molecular Descriptors*, Wiley-VCH, Weinheim, 2000, pp. 120–121.

SAŽETAK

Grafičke matrice u kemiji

Sonja Nikolić, Ante Miličević i Nenad Trinajstić

Prikazano je konstruiranje četiri tipa grafičkih matrica i dobivanje dvostrukih graf-teorijskih invarijanti. Postupak dobivanja dvostrukih graf-teorijskih invarijanti sastoji se od sljedećih koraka: (1) molekula se prikaže grafom, koji predstavlja njezin kostur bez vodikovih atoma; (2) numeriraju se čvorovi molekularnoga grafa; (3) konstruira se jedna od četiri vrste razmatranih grafičkih matrica pomoću odabranih podgrafova, koji se dobiju uklanjanjem čorova i/ili bridova iz grafa; (4) dobivanje numeričkih matrica iz grafičkih matrica zamjenom podgrafova s odabranim graf-teorijskim invarijantama; (5) primjena iste ili neke druge graf-teorijske invarijante na numeričku matricu i (6) dobivanje dvostruke graf-teorijske invarijante. Spomenuto je da se mnoge tzv. specijalne graf-teorijske matrice u literaturi mogu izvesti iz odgovarajućih grafičkih matrica. Kao primjeri dvostrukih invarijanta izvedena su dva deskriptora: Wiener-Wienerov i Hosoya-Wienerov indeks. Uporabivost ovih dvaju deskriptora u QSPR modeliranju ilustrirana je modelima za predviđanje vrelišta i steričke energije oktana. Dobiveni su modeli usporedljivi s najboljim modelima u literaturi.